International Journal of Civil Engineering and Technology (IJCIET)
Volume 7, Issue 1, Jan-Feb 2016, pp. 25-46, Article ID: IJCIET_07_01_003
Available online at
http://www.iaeme.com/IJCIET/issues.asp?JType=IJCIET&VType=7&IType=1
Journal Impact Factor (2016): 9.7820 (Calculated by GISI) www.jifactor.com
ISSN Print: 0976-6308 and ISSN Online: 0976-6316

SHEAR PERFORMANCE OF FIBER REINFORCED SELF COMPACTING CONCRETE DEEP BEAMS

Maher A. Adam
Associate Prof., Civil Eng. Dept, Shoubra Faculty of Eng., Benha University, Egypt

Mohamed Said
Assistant Prof., Civil Eng. Dept, Shoubra Faculty of Eng, Benha University, Egypt

Tamer. M. Elrakib
Associate Prof, Housing and Building National Research Center, Giza, Egypt

ABSTRACT

The self-compacting concrete (SCC) is the newest innovating category of high performance concrete. The shear behavior of Fiber Reinforced Self-Compacted Concrete (FRSCC) deep beams was investigated. The experimental program consisted of twelve simply supported beams tested up to failure under four-point load. The key parameters covered in this investigation were steel fibers ratios (0.0, 0.50, 0.75 & 1.00%) and the effective shear span to depth ratio; a/d that varied from 0.6 to 1.0. Also, the main flexure reinforcement ratio was variable (1.0, 1.60 and 2.20 percent). In addition, vertical and horizontal web reinforcement effect was investigated. The mid-span deflection, cracks, reinforcement and concrete strains of the tested beams were recorded and compared. Test results pointed out that the steel fibers enhanced the cracking load, ultimate capacity, displacement and energy absorption of the tested FRSCC deep beams. The utmost enhancement in the performance of deep beams was achieved with steel fibers content of 1.0% within the range of the test parameters. The enhancement in the ultimate capacity was 40%. The test results indicated that both vertical and horizontal web reinforcement are efficient in shear capacity enhancement of FRSCC deep beams. The ultimate shear capacity was increased by about 47% with increasing the longitudinal steel ratio from 1.0% to 2.2%. Maximum strain in the extreme compression fiber of concrete section was 0.0019 and achieved at specimen tested at a/d ratio of 0.6. A non-linear finite element analysis (NLFEA) model was constructed to simulate the shear behavior of tested beams, in terms of crack pattern and load deflection behavior. It can be concluded that a good agreement between the experimental and numerical

results was achieved. The ratio of the predicted to the experimental ultimate strength ranged between 0.98 and 1.04.

Key words: Self-compacting, Deep beams, NLFEA, Steel fibers, Shear Reinforcement.

Cite this Article: Maher A. Adam, Mohamed Said and Tamer. M. Elrakib. Shear Performance of Fiber Reinforced Self Compacting Concrete Deep Beams, *International Journal of Civil Engineering and Technology*, **7**(1), 2016, pp. 25-46.
http://www.iaeme.com/IJCIET/issues.asp?JType=IJCIET&VType=7&IType=1

1. INTRODUCTION

Reinforced concrete deep beams appear as common structural elements in many structures ranging from tall buildings to offshore gravity structures. They are used as load-transferring elements, such as transfer girders, pile caps, tanks, folded plates, and foundation walls. In buildings, a deep beam or transfer girder is used when a lower column is to be removed. Sometimes the full depth of the floor-to-floor height is used to transfer the high axial forces of columns above to the supporting columns below [1]. The high depth to span ratio causes non-linearity in the elastic flexural stress distribution over the beam depth and their strength is usually controlled by shear, rather than flexure [2]. ACI 318-14; [3] defines a deep beam as a structural element in which either the clear span is equal to or less than four times the overall depth, or the concentrated loads are applied within a distance equal to or less than two times the depth from the face of the support.

It has been widely shown that to increase the strength and reduce the brittleness of deep beams, it is necessary to increase the percentages of horizontal and vertical grids or to integrate or partially substitute the secondary shear steel reinforcements by using fiber reinforced concrete; FRC, as widely observed in the literature [4-8]. Reducing amounts of shear reinforcement in reinforced concrete deep beams can potentially reduce the congestion of reinforcing. In addition, steel fibers offer multi-directional reinforcement in concrete, simple detailing without congestion, and enhanced post cracking residual strength and ductility. The most common fibers utilized are end hook steel ones, and the best percentage for structural application is between 0.5% and 1.5% by volume of concrete. Lee [9] indicated that the steel fibers are more effective in improving the strength and ductility capacity than the stiffness and energy capacity of the specimens. Kimura et al. [10] pointed out that, the maximum flexural strength provided with steel fibers and the increases the fibers prevented the separation of the concrete and cover for columns under seismic actions. Therefore, the steel fibers may play the same role of horizontal and vertical web reinforcement.

Overcrowded arrangement of rebars in reinforced concrete members, such as deep beams, makes it difficult to compact concrete properly with the use of a mechanical vibrator. Self-compacting concrete (SCC) is a preferred substitution for conventional concrete where highly congested reinforcement is present or forms with complex shapes need to be filled. It is able to flow and consolidate under its own weight without the need for mechanical vibration (ACI 237R-07) [11]. The self-compacting concrete (SCC) was first developed by Okamura in 1986 [12, 13]. Although widespread application of SCC is still hindered by a lack of manuals and codes, it is expected that SCC will gain more popularity globally as a cost saving option. There have been a number of notable studies on structural shear behavior and performance

of RC structures made with SCC [14-17]. However, investigations on shear performance of SCC and FRSCC deep beams are inadequate [18-21].

This research work is aimed to study experimentally the shear behavior of SCC deep beams with and without steel fibers. The primary objective of the study is to investigate the effects of the variables covered in this investigation that are the steel fibers content; V_f, vertical and horizontal transverse reinforcement ratio, effective span-to-depth ratio; *a/d*, and the ratios of the main longitudinal reinforcement. In addition, numerical analysis using nonlinear finite element model (NLFEA) was conducted to evaluate the beams behavior employing ANSYS [22] software.

2. EXPERIMENTAL PROGRAM

2.1. Test specimens

The experimental program consisted of twelve specimens with concrete compressive strength about 27MPa.Each specimen tested in a four-point loading arrangement. All beams were constructed in the R.C. laboratory of the Housing and Building National Research Center. All beams were 150 mm wide, 450 mm deep and 1250mm long. The beams where simply supported over a span of 1.05 m. The shear span to depth ratio *a/d*, for specimens selected to be 0.60, 0.80 and 1.0.The steel fiber ratio in concrete mix was nil, 0.5%, 0.75% and 1.00%, respectively.

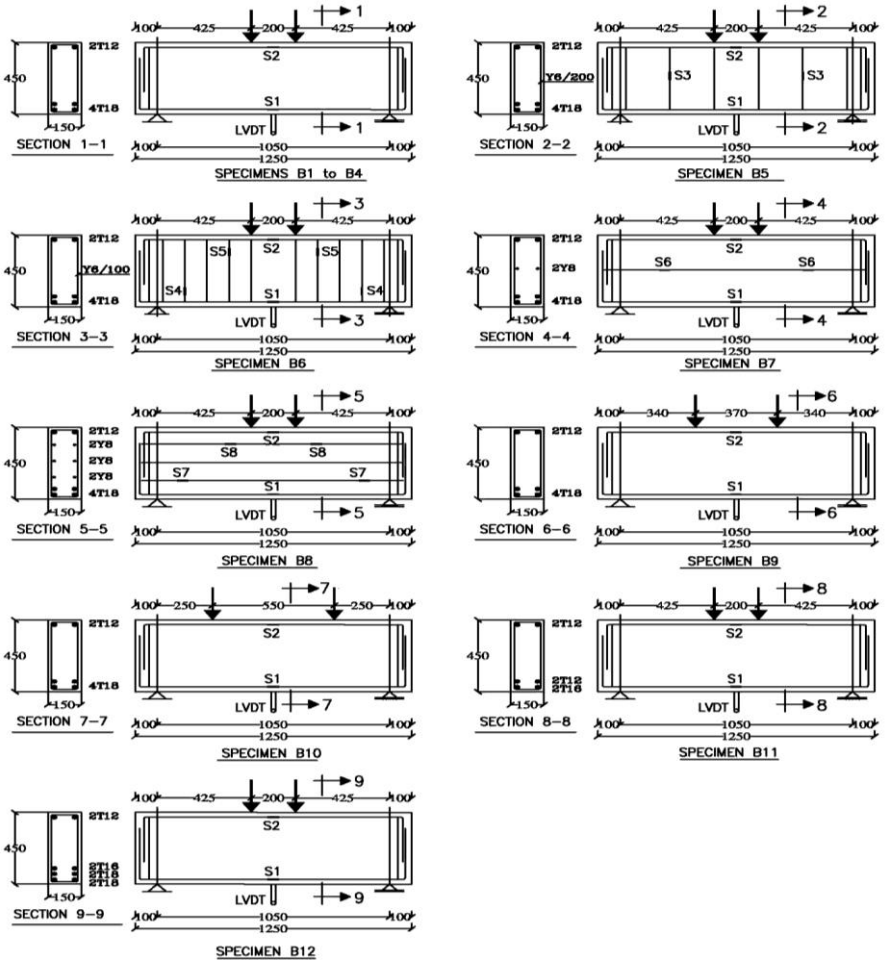

Figure 1 Test setup and details of tested beams

The fiber used in this study was end hook steel fibers with fiber length of 50 mm and diameter of 1.0 mm. High strength steel, grade 40/60, of 12, 16 and 18 mm diameter (denoted by T) was used in the experimental tests. Mild steel, grade 24/35, of 6 and 8 mm diameter (denoted by Y) was also used for horizontal and vertical stirrups. In order to investigate the shear behavior, the specimens were designed to fail in shear (i.e., the flexural capacity was designed to exceed the shear capacity). Typical concrete dimensions and reinforcement details and the setup of the test specimens are illustrated in Fig. 1. Table 1 summarizes the details of the test specimens.

Table 1 Details and parameters of test specimens

Group	Specimen	Concrete compressive strength(MPa)	*a/d*	Fiber content V_f%	Vertical stirrups	Horizontal stirrups	Bottom Rft.
G1	B1	27	1.0	0.00	-------	-------	4T18
	B2	27	1.0	0.50	-------	-------	4T18
	B3	27	1.0	0.75	-------	-------	4T18
	B4	27	1.0	1.00	-------	-------	4T18
G2	B5	27	1.0	1.00	Y6/200	-------	4T18
	B6	27	1.0	1.00	Y6/100	-------	4T18
G3	B7	27	1.0	1.00	-------	1Y8	4T18
	B8	27	1.0	1.00	-------	3Y8	4T18
G4	B9	27	0.80	1.00	-------	-------	4T18
	B10	27	0.60	1.00	-------	-------	4T18
G5	B11	27	1.0	1.00	-------	-------	2T16+ 2T12
	B12	27	1.0	1.00	-------	-------	4T18+ 2T16

2.2. Materials

The materials used throughout this program include aggregates, cement, fly ash; as cement replacement material, steel fibers, steel reinforcement and concrete admixture. Tests were carried out to determine the mechanical properties of the materials according to the Egyptian Code for Design and Construction of Reinforced Concrete Structures (ECCS-203-2003) Appendix 3 [23] (Guide of Experimental Tests for Concrete Material).Table 2 shows mix proportions by weight of the quantities needed for one cubic meter of concrete to achieve the target cube compressive strength. SCC can be largely affected by the characteristics of material sand mix proportion. Cementitious materials include Ordinary Portland Cement (OPC) type CEM I 42.5 N and fly ash Class F. The specific gravity of fly ash is 2.3 and its particle shape is spherical with 10% retention on 45-micron sieve. Coarse aggregate was natural siliceous gravel with 10mm maximum size. Viscosity Enhancing Agent (VEA), is the superplasticizer used in this experimental and its commercial name is Sika-Viscocrete 5-400.The steel fibers used were end hook fibers low carbon steel wire. The length of

fiber was 50mm. The diameter was 1mm and the tensile strength was about 1000 MPa.

Table 2 Mix proportions of concrete

MATERIAL	CEMENT (KG/M^3)	FLY ASH (KG/M^3)	DOLOMITE (KG/M^3)	SAND (KG/M^3)	WATER (LITER/M^3)	VISCOCRETE (VEA) (LITER/M^3)
QUANTITY	350	75	940	1000	206	7.5

High strength steel-deformed type; grade 40/60 of 10, 12 and 16 mm diameter, and mild steel-smooth type; grade 24/35 of 8 and 10 mm diameter were used in the experimental tests. Also, the actual area and unit weight were determined. Test results are given in Table 3.

Table 3 Mechanical properties of steel bars

Nominal diameter (mm)	Grade	Actual area (mm^2)	Yield strength (N/mm^2)	Ultimate strength (N/mm^2)	Elongation %
6	24/35	28	271	413	21.64
8	24/35	49	274	402	20.51
12	40/60	112	520	672	17.50
16	40/60	199	485	623	18.75
18	40/60	251	426	677	18.25

The slump flow test, T50 cm slump flow and L-box were carried out to investigate the material characteristics of fresh concrete. These tests were conducted to assess the flowability and flow rate of SCC in the absence of obstructions. The result of the slump flow is an indication of the filling ability of SCC. The test result of fresh concrete properties are shown in Table 4, these results are within the acceptable criteria for SCC given by ACI committee-363 [24] and indicate excellent deformability without blocking.

Table 4 Results of testing fresh SCC property in experimental work

Mix	Slump flow (mm)	T50 (sec)	L-box (H2/H1)
SCC	760	2.6	0.93
Limit ACI-363	650-800	2-5	0.8-1

2.3. Instrumentation and test procedure

Test specimens were instrumented to measure the applied load, mid-span deflection, strain at bottom reinforcement and strains of vertical and horizontal stirrups in the constant shear force region as shown in Fig. 1. A linear variable displacement transducer (LVDT) is used to record measurements at fixed time intervals. In addition; the bi-gauges were used to draw the surface concrete strain distribution along the beam depth. The load was distributed equally by a spreader beam to two points along the specimen. The test was continued after the ultimate load in order to

evaluate the post peak behavior of the tested beams. The development of cracks was marked along the sides of the specimens. Auxiliary specimens of cubes and prisms were tested on the same day of testing of FRSCC beams to determine the mean compressive strength and modulus of rupture of the concrete respectively.

3. TEST RESULTS

3.1. Cracking behavior

Typical behavior of beams is introduced through cracks pattern distributions recorded at applied load increments as shown in Fig. 2. The test beams were free of cracks in the early stages of loading. The initial shear crack inclined or diagonal crack was developed near the neutral axis in the shear span. With the increase in load, the shear crack propagated diagonally towards the top and bottom fiber of the beam with the development of additional shear and flexure cracks along the beam. All beam specimens failed in shear and shear cracks crossed the compression zone of beam section as clearly shown in Fig. 2.

For all specimens the shear cracks started without appearance of flexural cracks. For most of specimens without vertical and horizontal stirrups B1 to B4, B10 and B11, it was observed that a main crack was formed in the shear span region and gradually propagated towards the two loading points until failure occurred. In the other hand, other specimens had two nearly parallel diagonal cracks; in addition, a series of flexural cracks was formed at the bottom of specimens at zone between two point loads for these specimens.

The first shear crack in the middle of shear span, with an inclination angle was about 45^o, 51^o and 60^o for beams B4, B9 and B10, respectively. Generally, the first diagonal crack (shear crack) appears at the middle third of the diagonal region bounded by load and support positions at a loading level ranges between 53% and 57 % of the ultimate load for specimens with *a/d;* ratio equal to 1.0. For specimens B9 and B10 with *a/d;* ratio of 0.8 and 0.6 the first shear crack started at 49% and 45% of the ultimate load. Similar observation was recorded by CIRIA guide 2 [2]. Al-Khafaji *et al* [20] recorded that, for FRSCC deep beam strengthened with 0.8% steel fiber tested at *a/d;* ratio equal to 1.0 the diagonal shear crack started at 46% of the ultimate load. On the other hand, the first crack loads appeared at about 60% to 80% of the ultimate load for FRSCC deep beam tested by Shad and Modhera [25]. The influence of fiber content V_f; is very sensitive. The increase of V_f enhances the shear and tension resistances of concrete and plays an important role to bridge and arrest the cracks. This is the reason behind the delay of appearance of first flexural and diagonal shear cracks for FRSCC deep beams.

3.2. Mode of failure

In deep beams, significant part of load is transferred to support directly through compression struts formed between loads and supporting points. This mechanism of transferring load leads to the type of failure that is most common in deep beams.

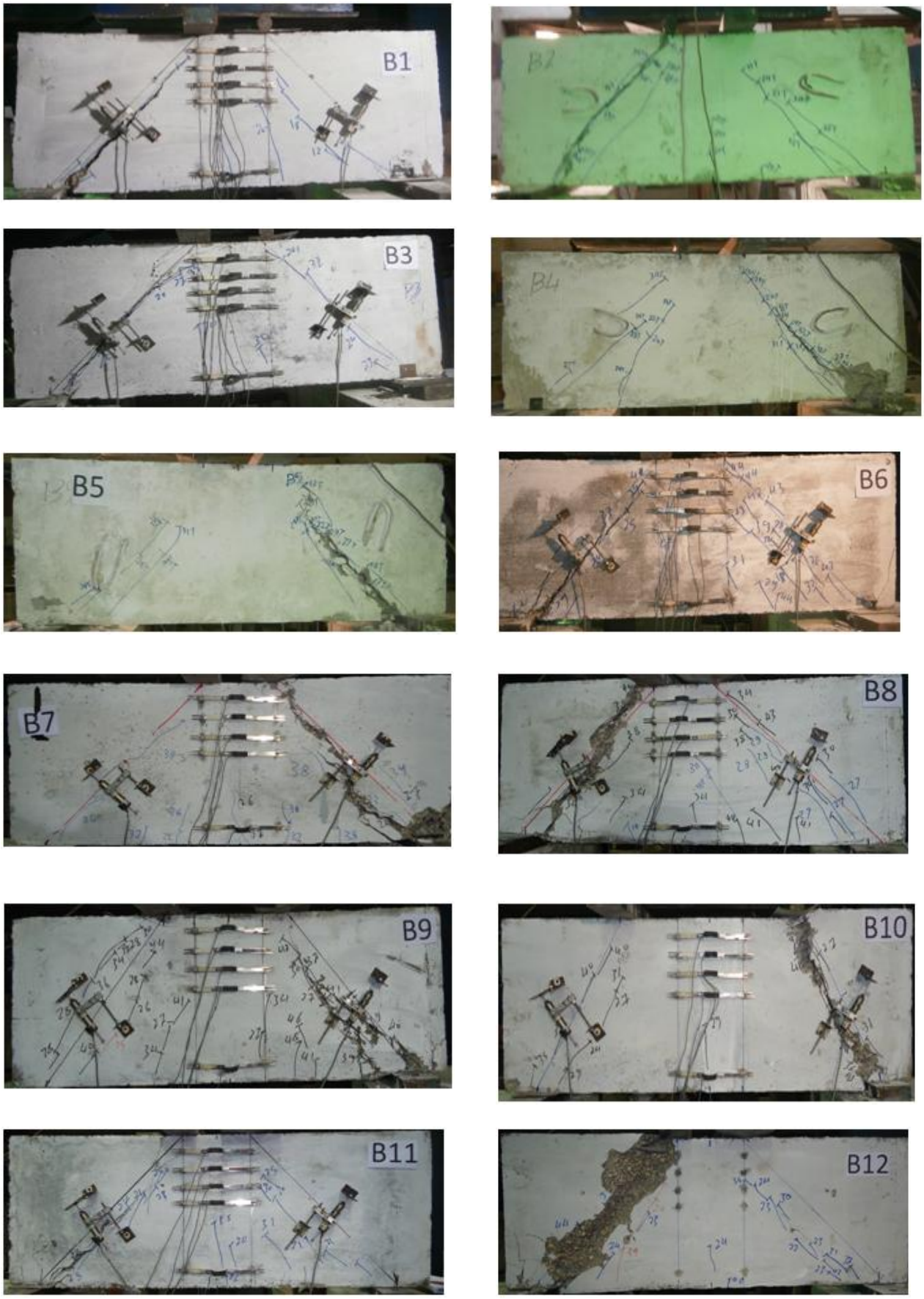

Figure 2 Crack Pattern of FRSCC deep beams

Table 5 Test results

Specimen	Experimental cracking level		Experimental ultimate level		NLFEA results		Absorbed energy (kN.mm)	Faliure mode
					Cracking	Ultimate		
	Δc (mm)	($P_{c\text{-}exp}$) (kN)	Δu (mm)	($P_{u\text{-}exp}$) (kN)	($P_{c\text{-}an}$) (kN)	($P_{u\text{-}an}$) (kN)		
B1	0.38	145.0	1.377	268.2	154.0	270.0	320.8	Shear splitting
B2	0.53	175.0	1.545	329.3	170.0	324.5	403.6	Shear splitting
B3	0.60	190.0	2.065	348.5	180.0	341.3	642.3	Shear splitting
B4	0.70	215.0	2.60	375.4	198.0	387.0	727.3	Shear splitting
B5	0.85	225.0	3.01	408.6	221.0	400.7	1035.9	Shear splitting
B6	1.01	250.0	3.67	443.8	240.0	452.0	1478.2	Shear crushing
B7	0.77	220.0	2.81	399.0	214.0	407.0	892.0	Shear crushing
B8	0.84	235.0	3.06	445.2	228.0	461.0	1073.4	Shear crushing
B9	0.78	250.0	3.57	514.4	234.0	512.0	1525.0	Shear crushing
B10	0.89	270.0	3.55	597.7	260.0	589.0	1653.7	Shear crushing
B11	0.79	170.0	2.02	302.4	158.0	297.0	476.8	Shear splitting
B12	0.75	250.0	2.77	441.7	249.0	435.0	1095.4	Shear crushing

All specimens exhibited the mode of shear failure as shown in Fig. 2. Specimens B1 to B5 and B11 exhibited a mode of shear failure characterized by splitting of the web concrete along the line joining the load pad and the beam support. The shear splitting failure occurred when a main crack developed to split the beam from top to bottom without crushing of concrete. For specimens failed with shear crushing, additional parallel diagonal cracks formed a series of concrete struts. One of the struts was failed by crushing between cracks, as shown in Fig.2. Failure of beams B6, B7 and B8 exhibited the role of horizontal and vertical steel stirrups in changing the mode of failure and increasing the ultimate load. Generally, at small *a/d* ratios the failure of the beams B9 and B10 was characterized by crushing of the web of the beams. As the shear span to effective depth ratio increased (*a/d*=1.0), the failure was characterized by splitting of the web of beam; B4.It is obvious that the significance of vertical compressive stresses on the shear response of the beam prevails on as the *a/d* ratio decreases. The experimental results pointed out that the shear behavior of SCC deep beams and the conventional vibrated concrete are dissimilar. The shear strength of FRSCC deep beam is less than conventional vibrated concrete deep beam due to lesser amount and smaller maximum size of coarse aggregate used in SCC. Evidently the interlock mechanism of coarse aggregate is weaker which represents an important part of the total shear strength parts for these members. Similar observation was recorded by Sultan [26].

3.3. Load-Deflection Relationship

The load mid-span deflection response was characterized by a linear uncracked response up to first diagonal cracking, followed by a nonlinear cracked response up to the peak load. Once the peak load was attained, sudden failure was observed for RC deepbeams.Fig.3 shows the load-deflection responses of five different series of beams. In general, deflections of deep beams are small compared with slender beams. As beam section height increases the stiffness of beam increases leading to brittle failure. The principal reason for incorporating fibers into a cement matrix is to improve the crack and deformation characteristics of the composite due to increases in tensile strength. As shown in Fig. 3a, the increase of steel fibers ratio; V_f leads to an increase in the ultimate load carrying capacity as a result of the enhanced post-cracking strength of steel fiber reinforced concrete. Experimental results of specimens with steel fibers given in table 5 reveal that the enhancement in the ultimate load was 23%, 30% and 40%, for specimens B2 with 0.50%, B3 with 0.75% and B4 with 1.00% steel fibers content, respectively. In addition, increasing the steel fibers content from 0.0 to 1.0 percent increased the ultimate displacement from 1.37 mm to 2.60 mm as shown in table 5.

As far as the specimens with fibers ratio of 1.0% are concerned, the load displacement shown in Fig. 3b proved that the ultimate load is enhanced significantly with increasing the vertical stirrups content. The maximum increase in the ultimate load was 18%, and in the ultimate displacement was 41% for specimens B6. On the other hand, Beam B8, with horizontal stirrups of R8/100 mm, showed improved ultimate load and post peak behavior. The ultimate load of this beam is higher than those of beams B7 (R8/200mm) and B4 (without horizontal stirrups) by about 12% and 19% respectively, as shown in Fig. 3c and table 5. Comparison of test results in Fig. 3d evinces the greet effect of shear span to depth ratio; *a/d*, on the shear capacity of test specimens. The ultimate shear capacity of Beams B9 and B10 was 1.37, and 1.60 times that of Beams B4. Concerning the longitudinal reinforcement ratio, the ultimate capacity was 302.4, 375.4 and 441.7 kN, and the ultimate displacement was2.02, 2.60 and 2.77 mm for beams provided with longitudinal steel ratio of 1.0%, 1.6% and 2.2%, respectively; as shown in Fig. 3e for specimens B11, B4 and B12.

3.4. Ductility

The brittle failure reduces the capacity of structural elements and considerably reduces the ductility and serviceability of the structure. The ability of dissipating the inelastic deformation energy is one of the significant factors for evaluating the ductility of the specimens. Based on Mohammadhassani *et al.* [27] the total dissipated energy was computed as the sum of the areas enclosed by the displacement. Referring to Fig. 3, as the displacement level increased, the energy dissipated increased. The energy dissipation for specimens provided with steel fibers was quite higher as clarified by the large areas enclosed by the load displacement of these specimens. The utmost energy dissipation was exhibited by the specimens strengthened using 1.0% steel fibers as shown in Table 5 and Fig. 4. Experimental results of specimens with steel fibers reveal that the increasing in the energy dissipation was 25%, 100% and 127%, for specimens with 0.50%, 0.75% and 1.0% steel fibers content, respectively; (B2, B3 and B4). Increasing the tension reinforcement ratio from 1.0 to 1.6 and 2.2 resulted in 52% and 130% increase in the absorbed energy, respectively. Also, as the spacing between horizontal and vertical stirrups decreased, the ductility of specimen increased.

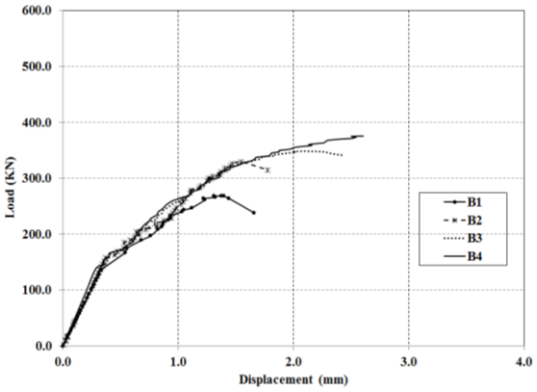

(3a)

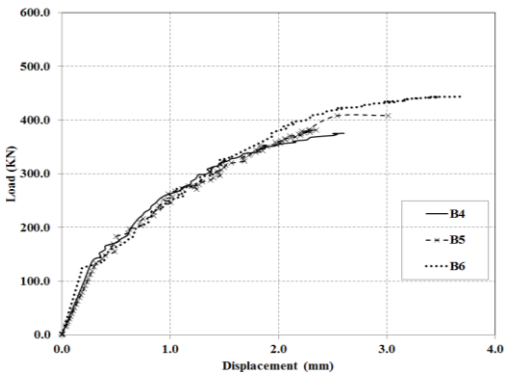

(3b)

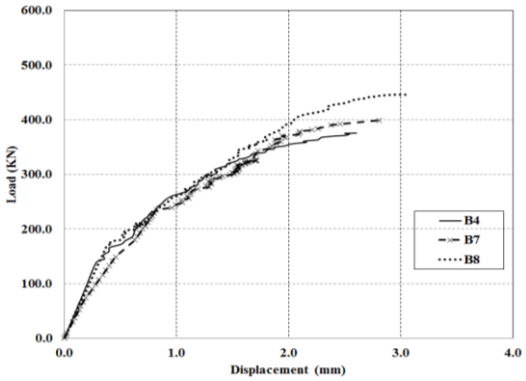

(3c)

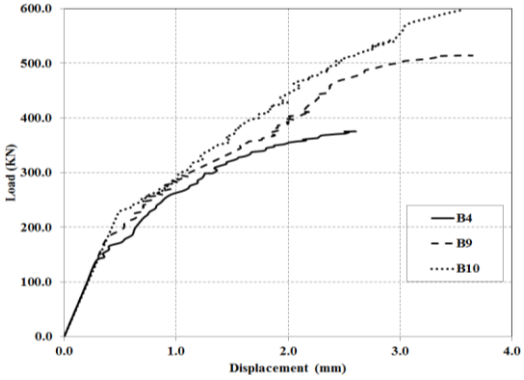

(3d)

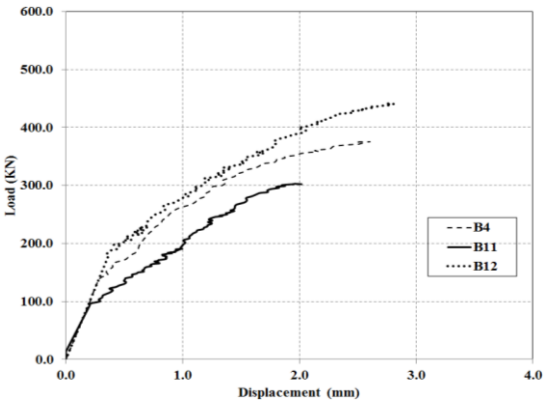

(3e)

Figure 3 Load-deflection relationship for tested specimens

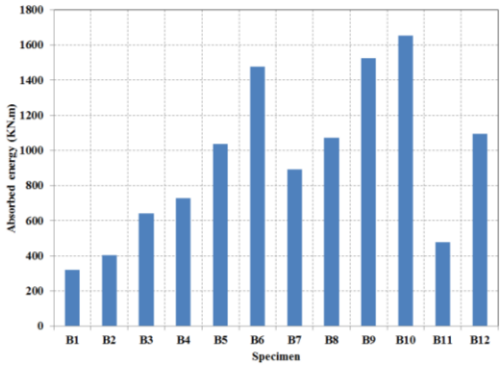

Figure 4 Absorbed energy of the tested specimens

3.5. Strains in reinforcement and concrete

Strain gauges were attached to the bottom steel bar of specimens to investigate the variation of strain in flexural reinforcement. These gauges were placed at mid-span of FRSCC specimens. Fig.5 shows the variation of measured strain of the specimens. The strain variation in longitudinal reinforcement was nearly similar for all tested specimens and the formation of a tie-action was observed. The strain readings increased rapidly in the vicinity of the first crack load. Eventually, the strain readings were increased with uniform rate until the failure load. The maximum strain in longitudinal tension bars was less than the yield value. The measured strains was ranged from 48% to 67% of yield strain. The strain gauges situated along the flexural steel of specimens B2 and B7 were inoperative. The measured strain in bottom reinforcement indicated that the flexure mode of failure was secured for all of the specimens to allow for shear mode of failure.

As shown in Fig 6, the strain in vertical stirrups was plotted. The strain in shear reinforcement stirrups was measured at the critical shear surface in order to gauge its effectiveness. Prior to cracking, the internal shear resistance was provided by the solid beam section. Once the inclined cracks occurred, the shear stirrups started to pick up strains, indicating shear resistance contribution by the vertical stirrups. The maximum strain in vertical stirrups was about 0.0016 and 0.00175 for specimen B5 and B6, respectively. The readings of strain in stirrups pointed out that the transverse reinforcement developed yielding before failure of specimens and also entered the strain hardening range exhibiting strains much higher than the yield strain which indicated that the stirrups were successful in resisting the shear stresses in FRSCC deep beams.

The concrete strain gauges measuring tension perpendicular to compression strut was recorded. Typical strain profiles for specimens B1 and B7 are drawn in Fig. 7.

The rate of increasing the tensile strain in concrete was very low till just before the formation of first shear crack, then, increased rapidly with load increase. From the data collected through strain and bi-gauges reading, the strain distribution through the height of beam section had been investigated and drawn. It was decided to present the strain distribution through the height of beam section at the ultimate load. Strain distributions along the height of mid-span of the twelve FRSCC deep beams tested as recorded by various bi-gauges at concrete surface are shown in Fig. 8. The stress and strain distribution in deep beams is nonlinear. The basic assumption for shallow beams that plane section remains plane after deformation, does not apply for deep beams. Deep beams exhibit lower strain in the extreme compression fiber. Maximum

recorded compressive strain was 0.0019 for specimens B10 tested at *a/d* ratio of 0.60. Mohammadhassani [28] recoded similar strain distribution profile. According to Fig. 8, 50%–78% of section height at mid-span was under tension. In addition, several neutral axes were obtained for the tested FRSCC deep beams. The neutral axis has a changeable depth till the failure. The study carried out by Ray [29] confirmed that there is more than one neutral axis before ultimate failure is reached. The area under tension decreases as tensile bar percentage increases as shown in Fig. 8e.

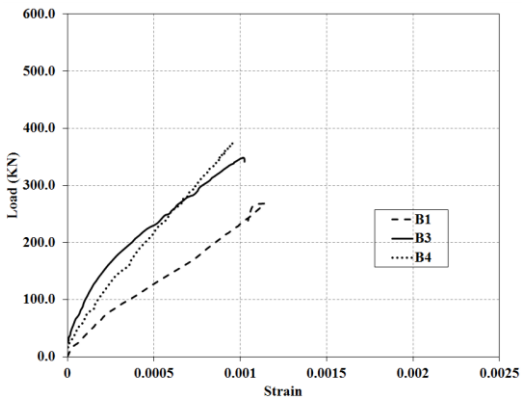

(5a)

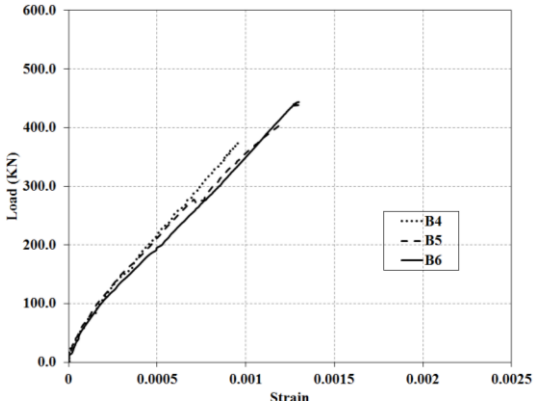

(5b)

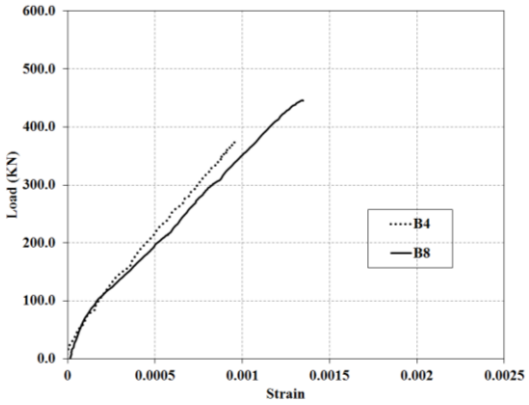

(5c)

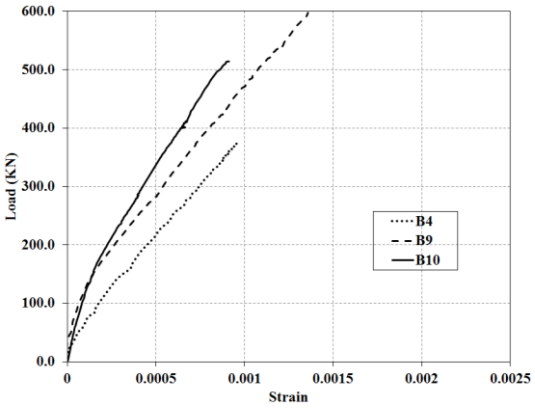

(5d)

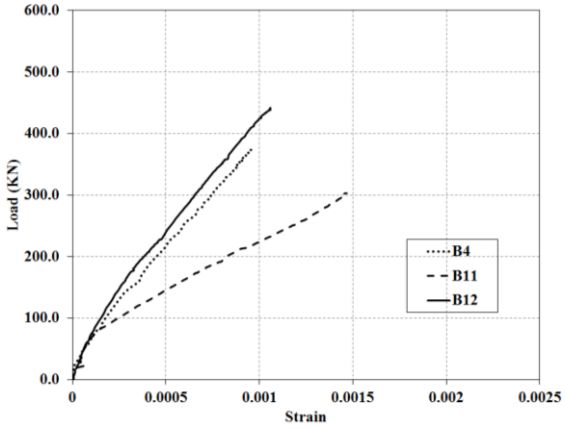

(5e)

Figure 5 Load-strains in the bottom reinforcement bars

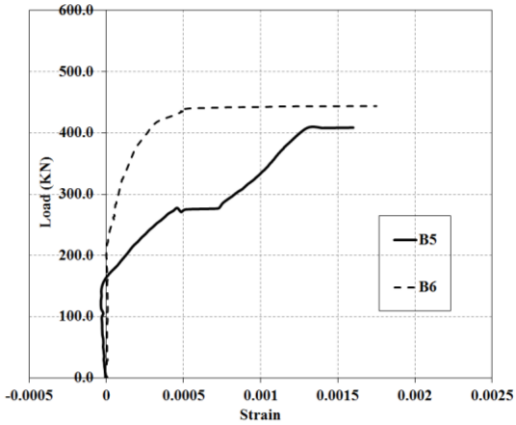

Figure 6 Load-strains in the vertical stirrups

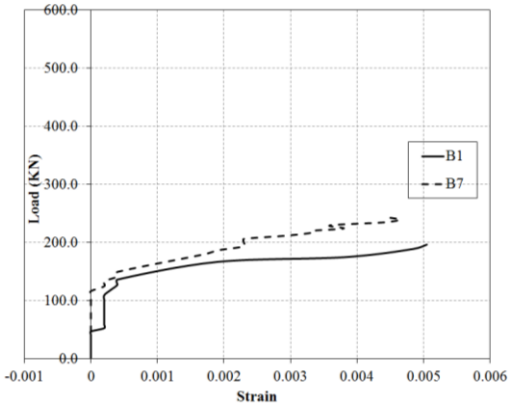

Figure 7 Load-strains (diagonal) in the concrete

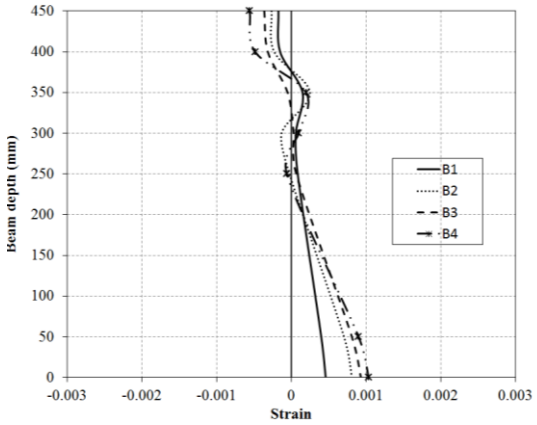

(8a)

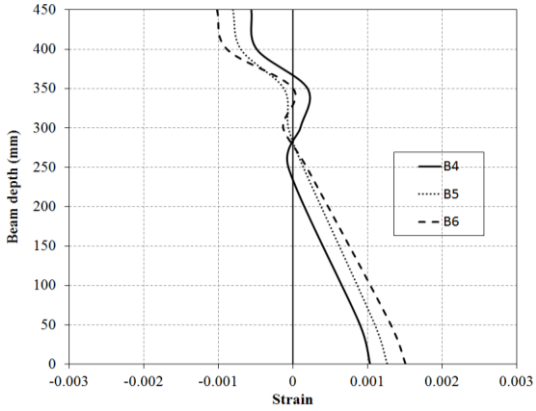

(8b)

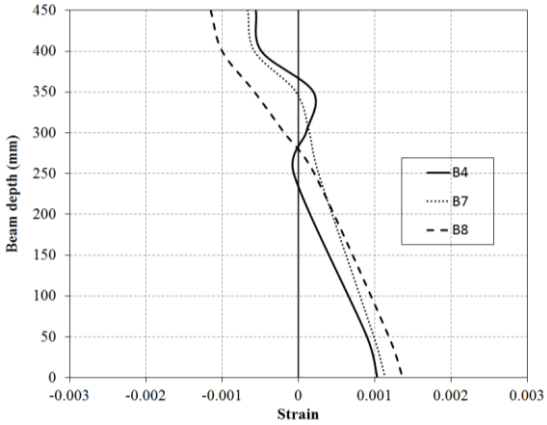

(8c)

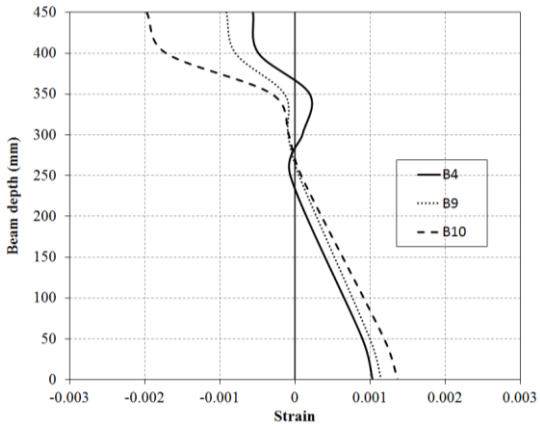

(8d)

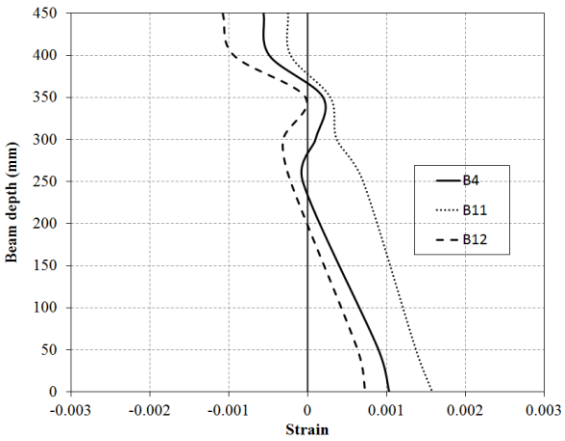

(8e)

Figure 8 Strain distribution of beams at ultimate load

4. EFFECT OF STUDIED PARAMETERS

4.1. Steel fibers content

Four specimens were tested to study the effect of the amount of steel fibers on the behavior of FRSCC deep beams. The test results show significant improvement in the cracking and ultimate load-carrying capacities of FRSCC deep beams. Compared to specimen B1, the increase in the cracking load was 21%, 31% and 78%, and in the ultimate load was 23%, 30% and 40% for specimens B2, B3 and B4, respectively, as given in table 5 and Fig. 3a. In addition, increasing the steel fibers content from 0.0 to 1.0 percent increased the ultimate displacement by about 86%. The estimated absorbed energy confirms the improvement in behavior of the specimens with steel fibers. The maximum enhancement in the absorbed energy was about 127%. The improvement in the cracking and ultimate load-carrying capacity is due to the fact that the steel fibers improve biaxial strength of FRSCC. In deep members, the strut and tie mechanism development is strongly influenced by the compressed strut biaxial strength, and the presence of fibers plays a fundamental role, as observed experimentally in the tested specimens [30].

4.2. Vertical web reinforcement

To investigate the effect of the vertical stirrups on the behavior of FRSCC deep beams, three beams were analyzed. All specimens had fibers content of 1.0%. Obviously, the vertical stirrups had no significant effect on the initial stiffness of specimens B4, B5 and B6 as depicted in Fig. 3b. Provision of the steel stirrups is shown to enhance the cracking and ultimate capacities of the tested beams. The enhancement increases with increasing the amount of stirrups and decreasing the spacing between them. Compared to the control Specimen B4, the increase in the cracking load was about 5% and 16% for B5 and B6, respectively. on the other hand, the maximum increasing in the ultimate load was about 19%.The absorbed energy of specimen B6 was about 2.0 times that of specimen B4. According to ACI 318 [3], minimum strut reinforcement needs to be provided to avoid splitting failure in struts. No clear consensus about the role of transverse reinforcement in bottle shaped struts. Catastrophic failure could be avoided by providing minimum transverse reinforcement [31].

4.3. Horizontal web reinforcement

Both the vertical and horizontal web reinforcement are efficient in resisting the shear capacity of deep beams, but the horizontal shear reinforcement is most effective when aligned perpendicular to the major axis of the diagonal crack [32]. Experimental results on three specimens; B4, B7 and B8 were investigated to demonstrate the effect of horizontal web reinforcement on the deep beam performance. The increase in the cracking and ultimate load due to presence of horizontal stirrups was about10% and 19%, respectively, for B8 as shown in Fig. 3c. Obviously, the horizontal and vertical web reinforcement had similar effective in providing shear strength for the tested beams. On the other hand, the horizontal web reinforcement changes the mode of failure from shear splitting to shear crushing, (see Fig. 2).

4.4. Shear span to effective depth ratio (a/d)

Reserve strength and normalized shear strength decreases when *a/d* increases. The shear span to effective depth ratio is highly influencing parameter of deep beams shear strength. Specimens B4, B9 and B10 were tested to investigate the effect of the shear span to depth ratio on FRSCC deep beams (see Fig. 3d). Decreasing the (*a/d*) ratio from 1.0 to 0.8 and 0.60 resulted in 16% and 26% increase in the cracking load, respectively, and resulted in 37% and 60% enhancement in the ultimate load, respectively, (see table 5). The maximum recorded compressive strain was about 0.002 for specimen B10 tested at *a/d*; ratio of 0.6.

4.5. Longitudinal steel reinforcement

Specimens B4, B11 and B12 were tested to demonstrate the effect of longitudinal reinforcement amount on the FRSCC deep beam performance. The load displacement was shown in Fig. 3e.The enhancement in the cracking and ultimate load was about 47%. The maximum improvement in the absorbed energy was 130% for specimen B12. Increase in the reinforcement ratio resulted in increase in ultimate load energy absorption and number of cracks. Beams with high tension reinforcement ratio endure the load beyond the elastic stage with less deflection. Clearly, compression strut fails when the tension capacity is high [27].

5. NON-LINEAR FINITE ELEMENTS ANALYSES

Finite elements method becomes a reliable tool in determining the stresses in the structure during linear and non-linear stage of loading. Application of the non-linear finite elements analysis (NLFEA) to a reinforced concrete structure is largely dependent on the stress-strain relationships, failure criteria, simulation of steel reinforcement and interaction between steel and concrete. NLFEA investigation of the shear behavior of the tested FRSCC deep beams was carried out using the finite element software "ANSYS 10.0" [22]. The load deflection curve is considered the key aspect in studying the FRSCC deep beams behavior as it involves many response parameters including beam ultimate strength, maximum deformation and cracking behavior. Therefore, correlating the load-deflection relationships of the analytical results with that of the experimental ones is considered an effective mean to verify the non-linear model. Numerous previous studies were carried to study shear behavior of reinforced concrete beams using ANSYS software [33, 34].

5.1. Finite element model

Non-linear finite elements analysis was carried out using a computer package "ANSYS 10.0". An 8-node solid element with three translational and additional rotational degrees of freedom at each node was chosen to idealize the concrete whereas a 2-node bar element was used to model the steel rebars. Specimens were typically discretized using 3000 of nearly equal-size 3-D isoparametric elements; Solid65 as shown in Fig. 9a. Both linear and non-linear behaviors of the concrete were considered. The concrete was assumed to be an isotropic material up to cracking stage and then to undergo plasticity. Cracking may take place in three orthogonal directions at each integration point. The stress-strain curve and behavior of SCC based on results from Maghsoudi and Arabpour [35] were adopted. The addition of steel fibers increases the strain corresponding to the peak stress but does not produce any significant change in the compressive strength. The steel fibers were represented by discrete model. The reinforcing bars were idealized using a 2-node bar (linear) element; Link8 as shown in Fig. 9b. In this study the main and web steel reinforcement are modeled as discrete and embedded, and the steel fiber modeled as smeared model.

To account for aggregate interlock dowel action and steel fibers content for FRSCC, the transfer of shear stresses is modeled numerically using a constant fraction shear retention model. Shear transfer coefficients were taken as 0.125, 0.150, 0.175 or 0.20 for open crack and 0.60, 0.625, 0.65 or 0.675 for closed crack, for fibers ratio of nil, 0.50, 0.75 and 1.0, respectively. A value of 0.6 for stress relaxation after cracking was considered in the analysis.

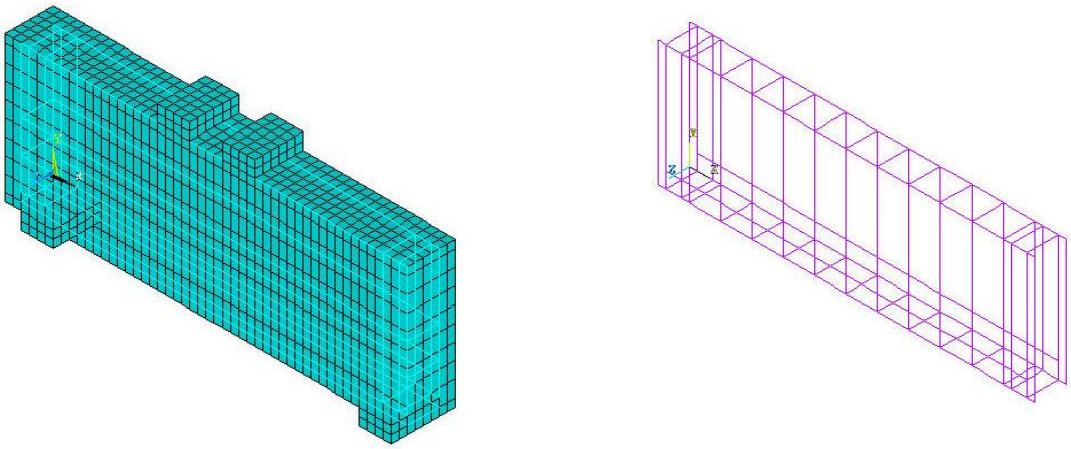

(9a) concrete element; Solid65; (9b) reinforcing bar element; Link8

Figure 9 Typical idealization of test beam

5.2. NLFEA predictions

A correlative study, based on the cracking and ultimate capacities, and load displacement, was conducted to verify the analytical model with the experimental results. Referring to Table 5, the predicted cracking loads; $P_{c\text{-}an}$ are shown to be in a good agreement with the experimental loads; $P_{c\text{-}exp}$ with a mean $P_{c\text{-}an}$ / $P_{c\text{-}exp}$ ratio of 0.97 and a standard deviation of 3.7%. The ratio of the predicted to experimental ultimate strength for the columns ranged between 0.98 and 1.04, with a mean value of 1.01 and a standard deviation of 2.0%. Implicitly, the analysis reflected the

significance of test parameters investigated on the load-carrying capacity. Furthermore, the analysis adequately reflected the enhancement in the ultimate capacity recorded for specimens provided with steel fibers. Output sample for NLFEA indicating the cracks propagation for beams B6 and B10 were given in Fig. 10. All beam specimens exhibited similar predicted patterns of crack development and propagation.

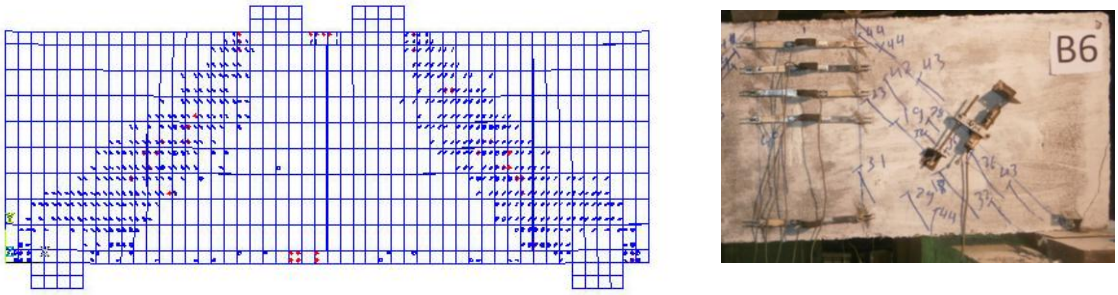

(10a) specimen B6

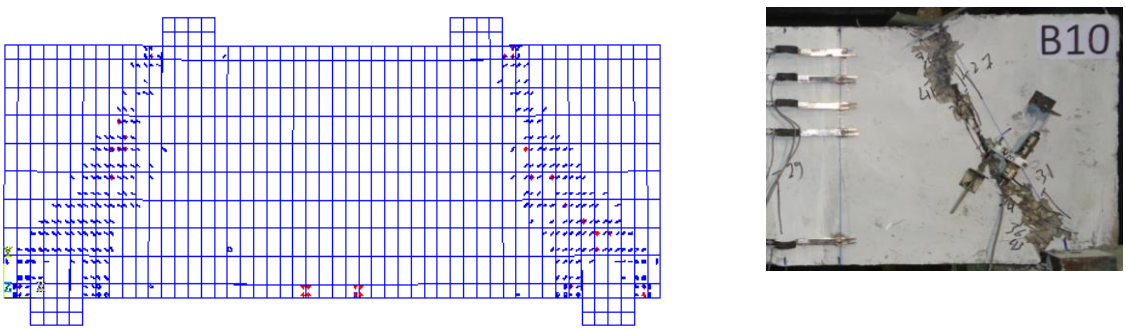

(10b) specimen B10

Figure 10 Cracks propagation for specimen B6 and B10

For specimen B12, the predicted shear and normal stresses distribution along the beam at ultimate load were presented in Fig. 11. The maximum analytical compressive and tensile stress for concrete was 20.5MPa and 2.3MPa, respectively. On the other hand, the shear stress in concrete was symmetrical and the maximum shear stress about 9.8 MPa.

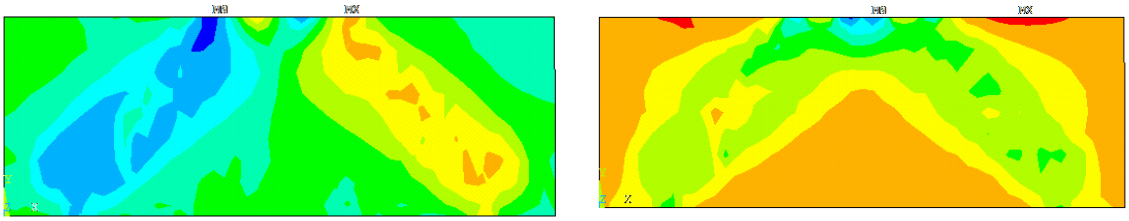

(11a) shear stress; (11b) normal stress

Figure 11 Concrete stress distribution for specimen B12 at ultimate load

Figure 12 shows the analytical results compared with the load deflection curve for all FRSCC deep beam specimens. The analytical results of the ultimate loads of most of the specimens were very close to the experimental results. In conclusion, to the range of the test parameters investigated, the application of non-linear finite elements model presented in this study yielded satisfactory cracking load, load-carrying capacity, and load-deflection response.

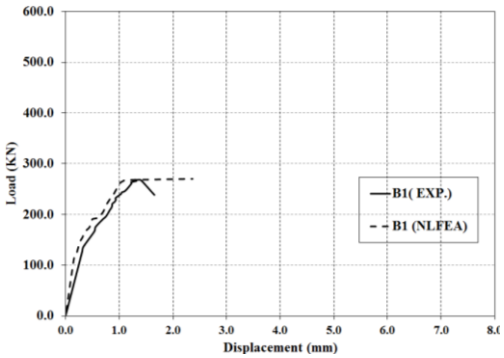

(12a) specimen B1

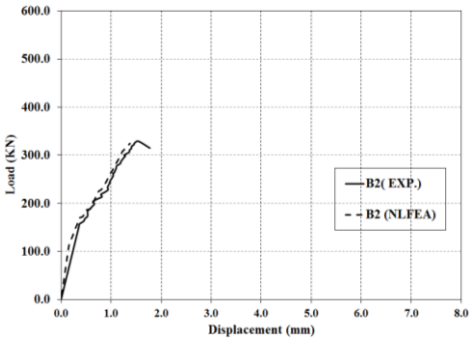

(12b) specimen B2

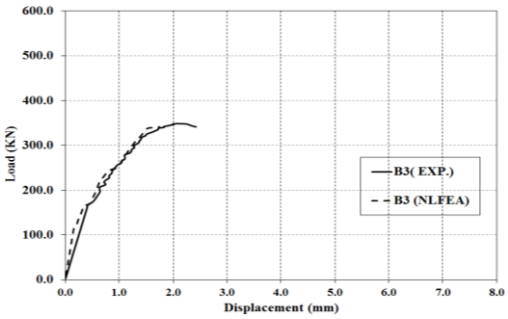

(12c) specimen B3

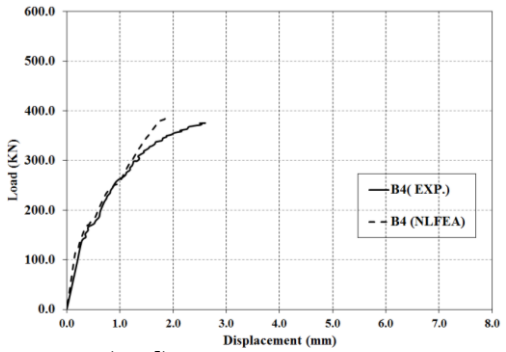

(12d) specimen B4

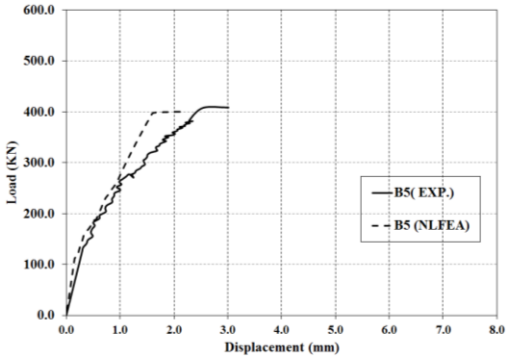

(12e) specimen B5

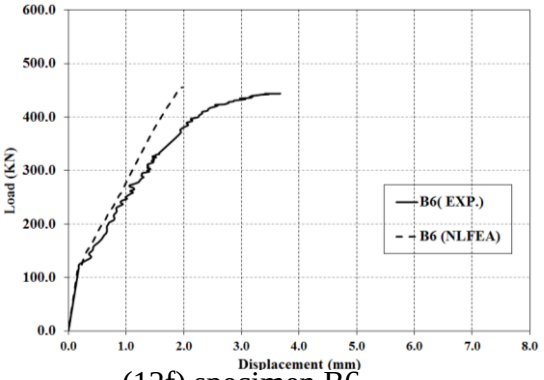

(12f) specimen B6

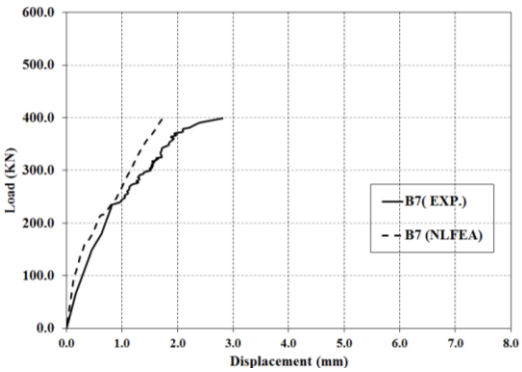

(12g) specimen B7

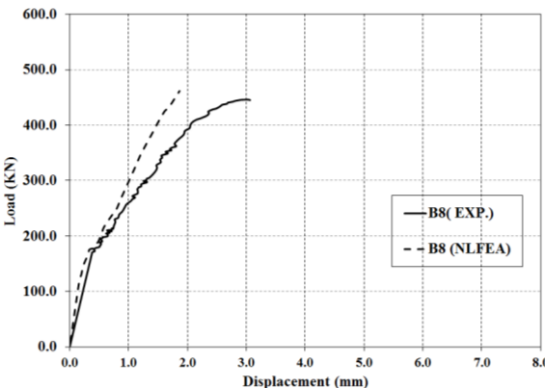

(12h) specimen B8

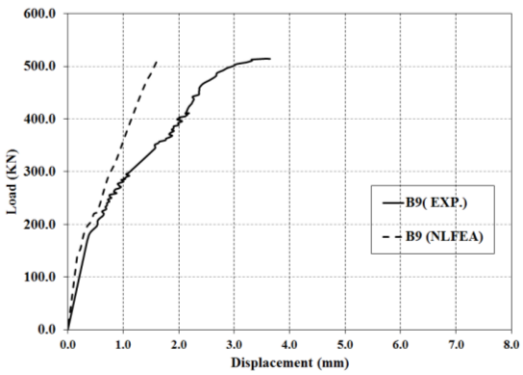

(12i) specimen B9

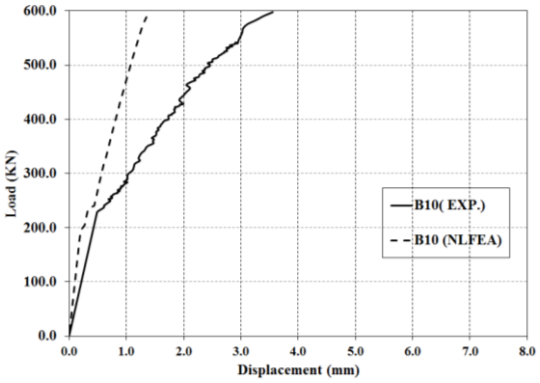

(12j) specimen B10

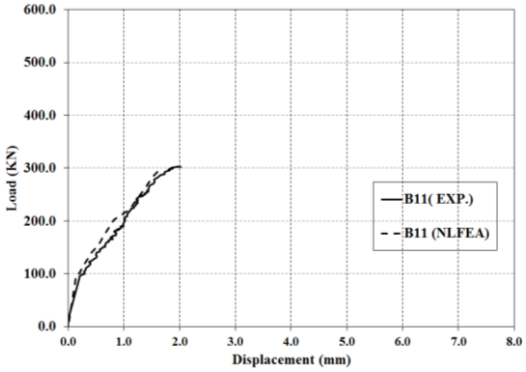

(12k) specimen B11

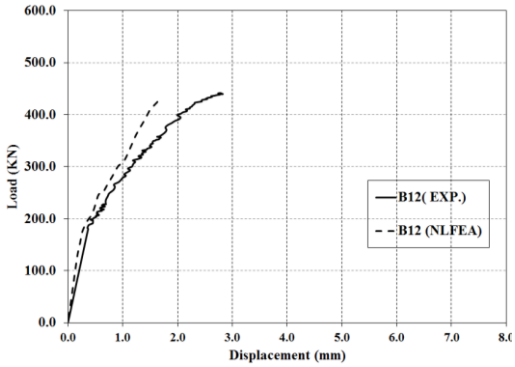

(12l) specimen B12

Figure 12 Experimental and NLFEA Load-deflection relationship for tested specimens

6. CONCLUSIONS

Based on the current investigation, the main findings may be summarized as follow:

- Provision of the steel fibers enhanced the cracking load, ultimate capacity, displacement and energy absorption of tested SCC deep beams. The utmost enhancement in the performance of beams was achieved with steel fibers content of 1.0% according to the range of the investigated parameters. The enhancement in the ultimate capacity and displacement was about 40% and 50%, respectively. The corresponding improvement in the energy absorption capacity was about 127%.
- The contribution of vertical web reinforcement to the shear capacity is proportional to the amount of shear reinforcement. The maximum increase in the shear capacity was about 19% for the range of the tested beams.
- The horizontal shear reinforcement can improve the shear strength of reinforced concrete deep beams as well as the vertical reinforcement. The load-carrying capacities of the beams with horizontal web reinforcement were 106% and 119% of that of the beam without horizontal web reinforcement.
- The failure of FRSCC deep beams without horizontal stirrups was classified as shear splitting failure whereas the corresponding beams with horizontal web reinforcement experienced a shear crushing mode of failure.

- Decreasing the shearing span to depth ratio increased the shear capacity of the concrete beams. Decreasing the shearing span to depth ratio from 1.0 to 0.6 led to increasing in the crack and failure load of the beam by 26% and 60 %, respectively.
- The ultimate shear capacity increases as the amount of main flexural steel increases pointing out the necessity of increasing the flexural reinforcement in the deep beam. The shear capacity increased with about 47% with increasing the longitudinal steel ratio from 1.0% to 2.2%.
- Strain distribution at the section height of mid span length is nonlinear with more than one neutral axis depth. Maximum measured strain in extreme compression fiber of concrete section is 0.0019.
- Application of non-linear finite elements model to test beams, yielded acceptable load-carrying capacities, cracking behavior and load displacement. The analysis adequately reflected the trend of experimental results.
- The experimental and analytical results pointed out that the deep beams work as a tied arch. The compression strut formed between the loading point and the support is under biaxial compression tension stresses. Beams with a shear span to depth ratio of less than 1.0 will work as tied arches provided that the main reinforcement is well anchored beyond the support.
- The construction of RC specimens can be time-consuming and labor-intensive due to the complicated detailing of reinforcing bars in contrast to the FRSCC specimens. The current findings represent good encouragement for the application engineers toward the use of FRSCC in deep beam structures.

REFERENCES

[1] Kong F. G., (2003), "Reinforced concrete deep beams," 2nd ed., Taylor & Francis, pp.2.

[2] CIRIA Guide 2, (1984),"The design of deep beams in reinforced concrete," London: Over Arup and Partners, and Construction Industry Research and Information Association; pp. 131.

[3] ACI Committee 318, (2014), “Building code requirements for reinforced concrete (ACI 318-14) and commentary (ACI 318R-14),” American Concrete Institute, Farmington Hills, Mich.

[4] Narayanan, R., and Darwish, I. Y. S., (1989), “Fiber concrete deep beams in shear,” ACI Structural Journal. 85, pp. 141-149.

[5] Mansur, M. A., and Ong, K. C. G., (1991), “Behavior of reinforced fiber concrete deep beams in shear,” ACI Structural Journal. 88, No. 1, pp. 98-105.

[6] Ward, R., and Hamza, A. M., (1992), “Steel and synthetic fibers as shear reinforcement,” ACI Structural Journal, V. 89, No. 5, pp. 499-508.

[7] Tan, K. H., Murugappan, K., and Parasivam, P., (1993), “Shear behavior of steel fiber reinforced concrete beams,” ACI Structural Journal. 90, No. 1, pp. 499-508.

[8] Campione, G., (2012), “Performance of steel fibrous reinforced concrete corbels subjected to vertical and horizontal loads,” ASCE Journal of Structural Engineering. 138, No. 2, pp. 235-246.

[9] Lee, H. H., (2007), “Shear strength and behavior of steel fiber reinforced concrete columns under cyclic loading,” Science Direct, Engineering Structures 29. pp. 1253-1262.

[10] Kimura, H., Kambayashi, A., and Takatsu, H., (2007), “Seismic behavior of 200 MPaultr-high-strength steel fiber reinforced concrete columns under varying axial load,” Journal of Advanced Concrete Technology, V. 5, No. 2, pp. 193-200.

[11] ACI Committee 237, (2007), "Self-consolidating concrete," ACI 237R-07, ACI Committee 237Report, American Concrete Institute, Farmington Hills, Michigan, pp. 32.

[12] Okamura, H., (1999), "Self-compacting high performance concrete, Tokyo: Social System Institute.

[13] Okamura, H., Maekawa, K., and Ozawa, K., (1998), High performance concrete," Tokyo: Gihoudou Publication.

[14] Choulli, Y., Marı´, A. R., and Cladera, A., (2008), Shear behavior of full-scale prestressed I-beams made with self compacting concrete," Materials and Structures, V. 41, pp. 131-141.

[15] Hassan, A. A. A., Hossain, K. M. A., and Lachemi, M., (2008), "Behavior of full-scale self-consolidating concrete beams in shear," Cement and Concrete Composites, V. 30, pp. 588-596.

[16] Hassan, A. A. A., Hossain, K. M. A., and Lachemi, M., (2010), "Structural assessment of corroded self-consolidating concrete beams," Engineering Structures, V. 32, pp. 874-885.

[17] Lachemi, M., Hassain, K. M. A., Lambros, V., Nkinamubanzi,P. C., and Bouzoubaa, N., (2005),"Self-compacting concrete in corporating new viscosity modifying admixtures," Cement and Concrete Research, V. 24, pp. 917-926.

[18] Hassan, S. A., (2012), "Behavior of reinforced concrete deep beams using self compacting concrete," PhD Thesis, University of Baghdad, Civil Department, Baghdad, Iraq, pp. 164.

[19] Mahmoud, K.Sh, (2012), Experimental study of the shear behavior of self compacted concrete T-beams, Journal of Engineering and Development, Vol. 16, No.1.

[20] Al-Khafaji, J., Al-Shaarbaf, I., and Wisam, W.H., (2014), Shear behavior of self compacting concrete deep beams, Journal of Engineering and Development, Vol. 18, No.2.

[21] Mohammadhassani, M., (2011), An experimental investigation on bending stiffness and neutral axis depth variation of over-reinforced high strength concrete beams," Nuclear Engineering. V. 241, pp. 2060-2067.

[22] ANSYS®, (2006), Engineering Analysis System User's Manual, Vol. 1 & 2, and Theoretical Manual", Revision 10.0, Swanson Analysis System Inc., Houston, Pennsylvania.

[23] ECCS-203, (2003), Egyptian code for design and construction of reinforced concrete Structures, Housing and Building Research Center, Egypt.

[24] ACI Committee 363, (1992), State-of-the-Art Report on High-Strength Concrete (ACI363R-92)," American Concrete Institute, Farmington Hills, Michigan, pp.55.

[25] Shah, D.L., and Modhera, C.D., (2010), Evalution of shear Strength of Self Compacting Concrete Deep Beam, International Journal of Advanced Engineering and Technology. V.I, Issue II, pp. 292-305.

[26] Sultan, W. H., (2013), "Behavior of steel fibers reinforced self compacting concrete deep beams under shear effect, PhD Thesis, University of Al-Mustansirya, Civil Department, Baghdad, Iraq, pp. 240.

[27] Mohammadhassani, M., Jumaat, M.Z., Ashour, A., and Jameel, M. An.,(2011), Failure modes and serviceability of high strength self compacting concrete deep beams, Engineering Failure Analysis 18, pp. 2272-2281

[28] Mohammadhassani, M., (2011), "Experimental and analytical study on HSSCC deep beams," PhD thesis, University of Malaya, Kuala Lumpur, Malaysia.

[29] Ray, SP, (2011), Behaviour and ultimate shear strength of reinforced concrete deep beams with and without opening in web, PhD thesis, Indian Institute of Technology, Kharagpur, India.

[30] Campione, G, (2012), Flexural behavior of steel fibrous reinforced concrete deep beams," ASCE Journal of Structural Engineering. V.138, No.2, 2012, pp. 235-246.

[31] Raj, J. L., and Rao, G. A., (2013), Performance of RC Deep Beams with Different Combinations of Web Reinforcement, Applied Mechanics and Materials, V. 343, pp. 21-26.

[32] Arabzadeh, A., Aghayari, R., and Rahai, A. R. (2011), "Investigation of experimental and analytical shear strength of reinforced concrete deep beams," International Journal of Civil Engineering. V. 9. No. 3. pp. 207-214.

[33] Said, M., Adam, M. A., Mahmoud, A. A., and Shanour A. S., (2016), Experimental and analytical shear evaluation of concrete beams reinforced with glass fiber reinforced polymers bars, Construction and Build. Material. V. 102. pp. 574-591.

[34] R. M. Sawant, Junaid Khan, Jabeen Khan and Satish Waykar. Behavior of High Strength Fiber Reinforced Concrete Under Shear, *International Journal of Civil Engineering and Technology*, **6**(4), 2015, pp. 46-54.

[35] Javaid Ahmad, Dr. Javed Ahmad Bhat and Umer Salam. Behavior of Timber Beams Provided with Flexural as Well as Shear Reinforcement In The Form of CFRP Strips, *International Journal of Advance Research in Engineering and Technology*, **4**(6), 2013, pp. 153-165.

[36] Majeed, H. Q., (2012), "Nonlinear finite element analysis of steel fiber reinforced concrete deep beams with and without opening," Journal of Engineering and Development, Vol. 18, No.2.

[37] Maghsoudi. A. A and Arabpour Dahooei. (2005), Effect of Nan scale Materials in Engineering Properties of Performance Self Compacting Concrete," 7th International Conf. In Civil Eng., University of Tarbiat Modares, Tehran. Iran.

[38] Dharane Sidramappa Shivashankar. Ferrocement Beams and Columns with X Shaped Shear Reinforcement and Stirrups, *International Journal of Civil Engineering and Technology*, **5**(7), 2015, pp. 172-175.